

RESEARCH ARTICLE | OCTOBER 27 2023

A simple, isotropic depolarized light source

K. D. Foreman  ; T. J. Gay 



Rev. Sci. Instrum. 94, 103104 (2023)

<https://doi.org/10.1063/5.0165103>



View
Online



Export
Citation

CrossMark



starting at
EUR 6.360,-

Grows with your experiment.
The MFLI Lock-in Amplifier.

Field-upgradeable options

- 5 MHz frequency extension
- Multi-frequency analysis
- PID controller
- Impedance analyzer

 [Zurich Instruments](#) [Find out more](#)

A simple, isotropic depolarized light source

Cite as: Rev. Sci. Instrum. 94, 103104 (2023); doi: 10.1063/5.0165103

Submitted: 26 June 2023 • Accepted: 5 October 2023 •

Published Online: 27 October 2023



View Online



Export Citation



CrossMark

K. D. Foreman^{a)}  and T. J. Gay 

AFFILIATIONS

Jorgensen Hall, University of Nebraska, Lincoln, Nebraska 68588-0299, USA

^{a)}Author to whom correspondence should be addressed: keith.foreman@unl.edu

ABSTRACT

Unpolarized light can be an important tool in optical experiments. Producing it, however, can prove to be a challenge. Natural sources of light that are commonly thought of as unpolarized are, in fact, either weakly polarized or not practical sources of light in a laboratory setting. Standard, commercially available light depolarizers produce unpolarized light only after the polarization state of the light across the diameter of the output beam has been averaged. Locally, such beams are highly polarized. In this work, we report a simple, low cost light depolarizer capable of producing light with a total polarization of less than 1% for a 15-mm diameter output beam. Based upon diffuse scattering, the light transmitted through the depolarizer discussed here produces only small polarizations locally, with the total polarization for a 1.25-mm diameter area being <6%. The effects of the depolarizer on the transmitted beam's intensity are also reported.

Published under an exclusive license by AIP Publishing. <https://doi.org/10.1063/5.0165103>

I. INTRODUCTION

Light, especially laser light, is an extremely important tool in many, if not most, physics experiments and their related applications. While polarized light is ubiquitous in optical research, unpolarized light may be required in applications using polarization-sensitive devices, such as Raman amplifiers¹ and diffraction gratings.²

Our need for an unpolarized light source and the motivation for the work presented here arise from the strict accuracy requirements of Accurate Electron Spin Optical Polarimetry (AESOP),³⁻⁵ which has been proposed as an absolute quantum standard for electron polarization measurements. In this technique, the beam of electrons whose polarization is to be measured excites noble gas atoms that subsequently fluoresce. By measuring the Stokes parameters of the emitted light, one determines, without the need for a calibrating measurement, the electron polarization. A preliminary goal in the development of this method is to determine the emitted light's Stokes parameters with an accuracy of 0.1% of their measured values. This requirement, in turn, necessitates an accurate and complete characterization of the optics used to measure the light's polarization.^{6,7}

Of particular importance is precise and accurate knowledge of the retardance of the waveplate used in the polarimeter.^{5,7} The achromatic retarders used in the AESOP optical polarimeter prototype are made of sheets of polymer sandwiched between glass.⁸

Should these retarders also linearly polarize the light transmitted through them, however weakly, this effect must be carefully quantified. One method to measure the linear dichroism of a retarder is to shine light through a pair of (ideally) identical retarders while rotating the downstream retarder and measure the intensity modulation of the transmitted light. Such a measurement is best performed using unpolarized input light. In this case, any transmitted intensity modulation can be attributed solely to the polarizing properties of the retarders. If the input light were itself polarized, the light transmitted through the first retarder would be in some arbitrary elliptical polarization state, making any intensity modulation more difficult to model.

Unfortunately, unpolarized light is difficult to produce. Sunlight, light from an incandescent bulb, and light from a flame are common examples of light that is generally thought of as "unpolarized." However, nascent sunlight is weakly polarized (on the order of 10^{-6}),⁹ and by the time it reaches the earth's surface, it can be up to 65% polarized.¹⁰ Similarly, light from an incandescent bulb must pass through the glass encasing the bulb and is thus weakly polarized, as we demonstrate below. Light from a flame is generally not considered to be a suitable light source for precise experiments.

Light depolarizers are commercially available^{11,12} at a cost on the order of 500 USD. These depolarizers, however, do not produce locally unpolarized light; the polarization of the throughput beam varies periodically across the beam's diameter with an

amplitude approaching unity. Small polarizations of the output beam result only when the local polarization is integrated over the beam's diameter.

In this work, we present a simple depolarizer capable of reducing the total polarization of highly polarized laser light to less than 1% across output beam diameters of 15 mm. It uses optical diffusers and costs less than 100 USD to build. Furthermore, because the depolarizing elements in our device are diffusers, the transmitted light is uniformly scattered. Thus, it has an isotropic polarization across the beam cross section. The output beam has low total local polarization, <6% for an integrated 1.25-mm diameter area, which does not vary more than 2% across its full output diameter of 15 mm. We are unaware of any previous quantitative discussion in the literature of such a device. The emphasis of this work is on the performance of the diffuser-based depolarizing elements. Measurements of the Stokes polarization parameters of the light before entering and after exiting the depolarizer are presented for several different light sources, input polarization states, and diffusing elements. The attenuation of throughput intensity and the spatial variation of the output polarization are also discussed.

II. DESIGN AND MEASUREMENTS

A. Depolarizer design

A scale drawing and photograph of the depolarizer we have developed are shown in Fig. 1. The housing that holds the depolarizing elements in place is made of a single piece of aluminum. In this work, we have studied three light sources: a 640-nm diode laser, a 405-nm diode laser, and an incandescent light bulb whose output is guided through a fiber bundle (Dolan-Jenner Industries, Inc. Fiber-Lite® Series 180 high-intensity illuminator) and then viewed through a 640-nm interference filter. One end of the aluminum housing is designed to slip over the end of the flexible fiber optic bundle used with the incandescent light. Two nylon set screws hold the fiber bundle termination sleeve in place. Alternately, laser light

can be sent directly into the depolarizer's cylindrical housing. A machined mechanical stop separates the end of the fiber bundle from the cavity that houses the depolarizing elements. Immediately downstream from the stop is a PTFE washer, followed by the first depolarizing element. Several depolarizing elements were studied, but all were 15-mm diameter disks. Next, a PTFE hollow tube separates the first depolarizing disk from a second one downstream. The tube holds the depolarizing disks in place and also serves to reduce reflections from the inner wall of the aluminum housing. In addition, the disks, together with the tube, define a cavity that can be filled with extra depolarizing media. Three nylon set screws hold the downstream depolarizing disk in place and secure the plane of the disk perpendicular to the optical axis.

The three depolarizing elements studied here were all purchased from Edmund Optics. The first is opal diffusing glass (part No. 46-645), the second is 220-grit ground diffusing glass (No. 45-652), and the third is "Broadband Hybrid" 120-grit semi-opaque white diffusing glass (No. 37-974). In this study, we had two depolarizing disks in place in the aluminum housing for all measurements, always of the same type.

B. Optical train and polarization measurements

Polarization measurements were made using the method described by Berry *et al.*¹³ Essentially, this process requires one to pass the light whose polarization state is to be measured through a rotatable optical retarding element and a fixed linear polarizer. The intensity of the light passing through these optical elements is measured as a function of the angular position of the fast axis of the optical retarder. Applying a fast Fourier transform algorithm to the intensity measurements, one is able to calculate the Stokes polarization parameters, P_1 , P_2 , and P_3 (which are equivalent to the parameters M/I , C/I , and S/I , respectively, used in Ref. 13). From these parameters, one can find the total polarization of the light, P_{tot} :

$$P_{tot} = \sqrt{P_1^2 + P_2^2 + P_3^2}. \quad (1)$$

To use the method described in Ref. 13, the depolarizing apparatus is placed in an optical train, as shown in Fig. 2. In the laser analysis configuration, the optical train was arranged as shown in Fig. 2(a). A 640-nm or 405-nm diode laser operating at 1 mW produced laser light that first passed through a beam splitter. The splitter sent part of the beam to a photodiode (PD 1), allowing the intensity recorded by the throughput photodiode (PD 2) to be normalized in the event of power fluctuations in the laser output. The light then passed through a linear polarizer (LP 1) and retarder ($\lambda/4$ 1). These two components are mounted in computer-controlled rotatable mounts that allow any polarization state of the light entering the depolarizer to be selected.

The polarized light then enters the depolarizer. The depolarization occurs primarily through the mechanism of diffusive multiple scattering, mostly in the depolarizing disks but also from the walls of the depolarizer housing itself and any material placed between the depolarizing disks. To define the depolarizer's output beam following this multiple scattering, a variable-diameter iris is placed immediately downstream of the depolarizer and upstream of the analysis polarimeter and photodiode detector (PD 2). Most of the measurements described below were taken with an output beam

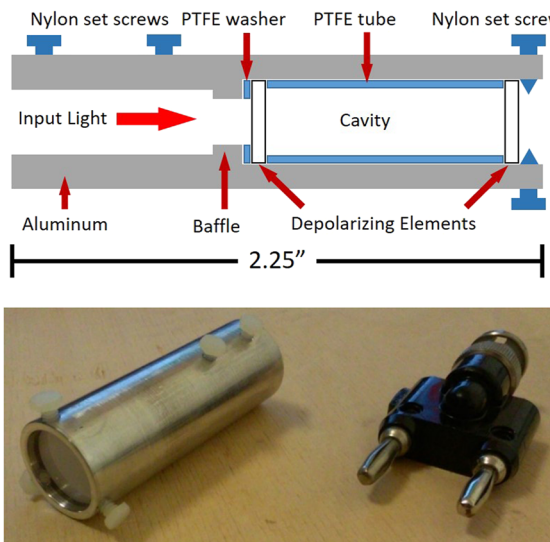


FIG. 1. Sectional view of the depolarizer (top) and a photograph of it (bottom).

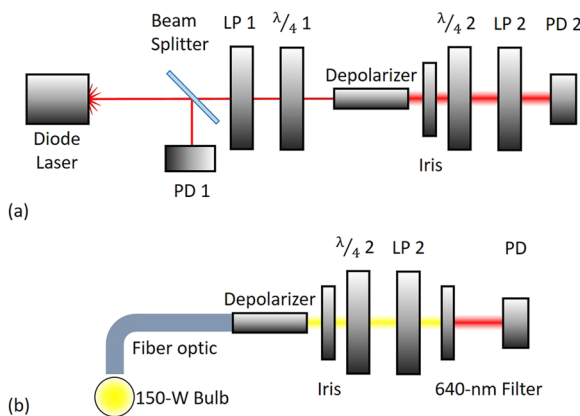


FIG. 2. Optical train design for measurements of depolarized laser light (a) and depolarized white (incandescent) light (b).

diameter of 15 mm. The analyzing optics used to measure the polarization state of light exiting the depolarizer consist of a retarder ($\lambda/4$ 2) and a linear polarizer (LP 2). These two components are also mounted on computer-controlled rotatable mounts.

Both LP 1 and LP 2 were purchased from Thorlabs (part No. LPVISE200-A) and are highly polarizing elements (polarization efficiencies measured to be >99.9%) with operating wavelengths spanning the visible spectrum. When the light source in the optical train was the 640-nm diode laser or the incandescent light bulb, both $\lambda/4$ 1 and $\lambda/4$ 2 were precision achromatic retarders purchased from Meadowlark Optics (part No. AQM-250-0720-C) with an operable range from 630 to 835 nm. At 640 nm, the measured retardance of $\lambda/4$ 1 and $\lambda/4$ 2 is 91.19(1) $^{\circ}$ and 88.17(1) $^{\circ}$, respectively. When the light source was the 405-nm diode laser, both $\lambda/4$ 1 and $\lambda/4$ 2 were precision retarders also purchased from Meadowlark Optics (part No. NQM-250-0389-C) that are quarter-wave plates at 389 nm and have a retardance of 86.4(1) $^{\circ}$ at 405 nm.

Measurements were also made with white light produced by a 150-W incandescent bulb in a “gooseneck” illuminator. For these measurements, the optical train was configured as shown in Fig. 2(b). In this configuration, the diode laser, beam splitter, and polarization-state-defining optics are removed and replaced by the fiber optic guiding the light from the illuminator. The depolarizer is mounted directly on the end of the fiber line using the nylon set screws. However, since typical spectroscopic experiments do not sample broadband light and since the analyzing retarders are best suited for the specific wavelength(s) mentioned above, a 640-nm filter is placed immediately upstream of the photodiode (PD).

III. PERFORMANCE

A. Integrated depolarization

Ultimately, the AESOP experiment plans to measure fluorescent light from several specific atomic transitions, one of which is the Ne $3s^3P_2-3p^3D_3$ 640-nm line. For this reason, the depolarizer was tested using a 640-nm diode laser with the optical train configured as shown in Fig. 2(a). All three depolarizing elements were tested for both linearly and circularly polarized input light, while initially, the cavity in the depolarizer remained empty apart from the PTFE tube lining. The results of these measurements are summarized in Table I below. First, the polarization state of the light was measured before entering the depolarizer (the “input light”). For the linearly polarized input light, the normalized Stokes vector was

$$\vec{S}_{input} = \begin{pmatrix} 1 \\ 0.999\,471(5) \\ -0.000\,546(11) \\ 0.001\,354(9) \end{pmatrix}.$$

From Eq. (1), the total polarization, P_{tot} , of this input light is 0.999 472(5). With this linearly polarized light, the effect of the

TABLE I. Depolarization measurements for various configurations of the depolarizer using linearly and circularly polarized 640-nm laser light as the source.

Depolarizing Element	Cavity	Linear Input, $P_{tot} = 0.999472(5)$	Circular Input, $P_{tot} = 0.999943(9)$
		P_{tot} Output	P_{tot} Output
Opal	PTFE	0.006141(25)	0.009860(14)
Opal – Rotated	PTFE	0.006959(21)	0.009526(14)
Ground	PTFE	0.966091(3)	0.951327(12)
Ground – Rotated	PTFE	0.965449(4)	0.951191(10)
Broadband	PTFE	0.008279(36)	0.015687(26)
Broadband – Rotated	PTFE	0.010143(39)	0.012285(23)
Opal	PTFE with Kimwipe®	0.120767(375)	0.239665(175)
Opal	Stained PTFE	0.017556(21)	0.022830(13)
Sandblasted Opal	Stained PTFE	0.027467(24)	0.021213(16)

depolarizer on the full output (“integrated”) 15-mm diameter beam was then measured. The normalized Stokes vectors of the depolarized light exiting the depolarizer when using the opal diffusing glass, ground diffusing glass, and broadband diffusing glass, respectively, were measured to be

$$\vec{S}_{\text{opal}} = \begin{pmatrix} 1 \\ 0.002\,037(16) \\ -0.005\,488(20) \\ 0.001\,856(7) \end{pmatrix},$$

$$\vec{S}_{\text{ground}} = \begin{pmatrix} 1 \\ 0.965\,966(3) \\ 0.015\,321(6) \\ 0.002\,452(4) \end{pmatrix},$$

and

$$\vec{S}_{\text{broadband}} = \begin{pmatrix} 1 \\ 0.005\,282(24) \\ -0.006\,103(25) \\ 0.001\,841(12) \end{pmatrix}.$$

These Stokes vectors yield total polarizations: $P_{\text{tot}} = 0.006\,141(25)$, $0.966\,091(3)$, and $0.008\,279(36)$, respectively. Since our primary concern is the production of unpolarized light, P_{tot} is the figure of merit that best quantifies the performance of the depolarizing elements. Thus, only P_{tot} is reported for these measurements, although the complete normalized Stokes vector for every measurement discussed here can be found in the supplementary material accompanying this work.

With each pair of depolarizing elements, the output P_{tot} value was measured twice: once after the disks were placed in the depolarizer, as shown in Fig. 1(a), and again after the downstream disk was rotated about the optical axis by 90° (denoted as “Rotated” in Table I). For the opal and ground glass diffusers, P_{tot} for these two measurements differed by a few hundredths of a percent, while the change in disk orientation of the broadband diffuser resulted in a

much larger change. We attribute these differences to local defects and anisotropies in the material introduced during the manufacturing of the disks. From these results, we conclude that the opal diffusing glass is the most effective depolarizing element, reducing the total polarization of the highly polarized input light to less than 1% across the full area of the output beam in all measurements. Surprisingly, the ground glass was largely ineffective at depolarizing the light, reducing the total polarization to no less than 95% in any of the measurements.

As shown in Fig. 1(a), the depolarizer was designed such that the two depolarizing elements defined a cavity inside which additional depolarizing material could be placed. With the best performing depolarizing elements tested, the opal glass diffusers, we performed another measurement of the depolarizing effects on both linearly and circularly polarized input light when the cavity was filled with a crumpled Kimwipe®, a fairly coarse-grained white laboratory cleaning tissue. These results are also shown in Table I. Interestingly, when the cavity of the depolarizer was filled with a randomly patterned, coarse material, the effectiveness of the depolarizer was reduced—that is, P_{tot} for the transmitted light was significantly greater with the material in the cavity compared to when the cavity was empty. It is possible that by stuffing the cavity with Kimwipe®, the layered folds in the material introduce relatively flat reflective surfaces that reduce the effectiveness of the depolarizing elements.

Additional modifications were made to the depolarizer and tested with the opal disks in an effort to further enhance the system’s depolarizing performance. The PTFE tube cavity liner was “sooted” by holding it near an acetylene torch and collecting the soot on the tube. The large pieces of soot were then washed away, yielding a PTFE tube that was stained a light gray matte color (denoted as “stained PTFE” in Table I). In addition, a pair of opal diffusers were sandblasted to roughen the otherwise shiny surface of the disk. The measured polarization of the transmitted light using smooth opal diffusers and the stained cavity liner increased to about 2%, up from less than 1% when using the clean, seemingly more reflective PTFE cavity liner. The sandblasted opal diffusers with the stained PTFE produced total polarization between 2% and 3%.

With the best performing combination from the above measurements, smooth opal glass with an empty, unstained PTFE-tube-lined depolarizer cavity, we next measured depolarization effects using a linearly and circularly polarized 405-nm diode laser source light. (This wavelength was chosen because it is at the other end of

TABLE II. Depolarization measurements for various configurations of the depolarizer using linearly and circularly polarized 405-nm laser light as the source.

Depolarizing Element	Cavity	Linear Input, $P_{\text{tot}} = 0.997132(4)$	Circular Input, $P_{\text{tot}} = 0.998556(11)$
		P_{tot} Output	P_{tot} Output
Opal	PTFE	0.028950(447)	0.039736(232)
Opal – Rotated	PTFE	0.035771(415)	0.034642(223)
Opal	Stained PTFE	0.022840(491)	0.036043(267)
Sandblasted Opal	Stained PTFE	0.016412(898)	0.041270(435)

TABLE III. Depolarization measurements for various configurations of the depolarizer using incandescent white light from a "gooseneck" illuminator as the source and viewed through a 640-nm filter.

Depolarizing Element	Cavity	Input Light, $P_{tot} = 0.009170(386)$	P_{tot} Output
Opal	PTFE	0.005828(440)	
Sandblasted Opal	PTFE	0.002917(391)	
Opal	Stained PTFE	0.006184(430)	
Sandblasted Opal	Stained PTFE	0.004656(435)	

the visible light spectrum and is close to another AESOP polarimetric transition: the He 2^3S-3^3P 389-nm line.) In addition, the stained cavity liner was also tested with both smooth and sandblasted opal diffusers. The results, as well as the total polarization of the 405-nm linearly and circularly polarized input light, are shown in Table II. Generally, the depolarizing effect using the 405-nm light is not as large as that achieved using the 640-nm light source, yielding total polarizations as high as 4.1%. The stained cavity liner and sandblasted disks had a marginal effect on the total polarization of the transmitted light.

The last light source tested was the 150-W incandescent bulb coupled with the fiber bundle, viewed through a 640-nm filter. As with the laser light, the polarization state of the light as it first entered the depolarizer was measured using the optical train shown in Fig. 2(b), but with the depolarizer removed from the end of the fiber line. Then, with the depolarizer back in position, the depolarization effect of the best performer from the previous measurements, the opal diffuser, was tested in various configurations. The results are shown in Table III.

First, we point out that the 640-nm light leaving the fiber bundle is about ~1% polarized. While the light from an incandescent bulb filament is often considered to be unpolarized, its passage through the glass of the bulb and subsequently through the optical fibers invariably produces a low level of polarization. Our depolarizer reduced this total polarization to less than 0.5% across the 15-mm output beam diameter when using sandblasted opal.

B. Spatial variations of the output polarization

Documentation made available by the manufacturers of commercial depolarizers indicate that the output beam from these devices is highly polarized locally and that the polarization across the beam cross section is highly anisotropic. For example, one commercially available liquid-crystal polymer (LCP) depolarizer¹¹ produces a beam with sinusoidally oscillating Stokes parameters across one diameter of the beam cross section for which the local maxima of P_{tot} approach unity. Documentation for this particular depolarizer indicates that for polarized input light at 532 nm, the total polarization of the output beam is still ~14% across a beam size of 1 mm.

To measure the effect of integration area on P_{tot} for the depolarizer presented in this work, we used the linearly polarized 640-nm laser source light and the best performer from the trials using that source: the smooth opal glass diffusers with a clean PTFE tube. The iris immediately downstream of the depolarizer shown in Fig. 2 is now partially closed such that the output beam is narrowed and a

smaller beam cross section can be sampled, while the center of the aperture remains on the principle axis. With this iris, the polarization of beams with cross section diameters of 12, 9, 6, 3, and 1.25 mm was measured. The 1.25-mm diameter aperture is the smallest size that produces a strong enough signal above the background that can still be reliably measured. The total polarization of these smaller sampling areas, together with the total integrated polarization of the unobstructed beam of 15-mm diameter reported in Table I above, is shown in Fig. 3. The complete normalized Stokes vectors for these measurements are included in the supplementary material.

As with the commercially available depolarizers, we see an increase in the total polarization of the output beam as the cross-sectional area of integration is decreased. However, even with a beam size of 1.25 mm, the total polarization of the output beam is less than 6%. (Recall that the polarization of the input beam is 99.9%.) The size of particles in opal glass ranges from 0.4 to 1.3 μm ,¹⁴ and so we speculate that for high input polarizations, the output polarization would be large across beam sizes of this order of length. Unfortunately, this cannot be tested easily as the signal passing through an aperture of this size would be too weak to detect with our apparatus.

Since the depolarizing elements are very good diffusers, we expect the polarization of the output beam to be isotropic across the cross section of the beam compared to the highly anisotropic commercially available devices (e.g., Ref. 11). To investigate the spatial uniformity of the cross section of the output beam, we set the downstream iris to an aperture diameter of 1.25 mm. The aperture is then used to sample the light leaving the depolarizer at the 12 o'clock, 3 o'clock, 6 o'clock, and 9 o'clock positions, ~7.5 mm from the beam center. The normalized Stokes parameters and total polarization of the output beam at these positions, together with the center position (the first data point in Fig. 3), are shown in Table IV.

The total polarization when integrating across a 1.25-mm diameter area of the output beam at different off-axis locations is between ~2.8% and ~5.6%, compared to the ~14% total polarization of a 1-mm beam size for the commercial LCP device. As expected, the algebraic signs of the individual normalized Stokes parameters change at these various positions, indicating that the polarization

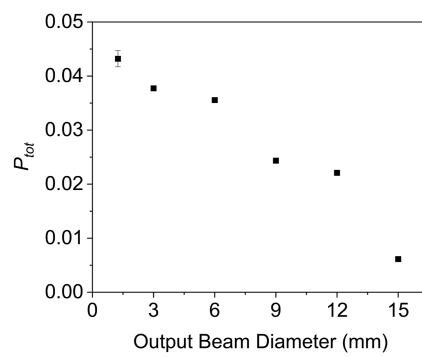


FIG. 3. Total integrated polarization of the output beam as a function of the beam size (diameter) defined by the iris immediately downstream of the depolarizer.

TABLE IV. Normalized Stokes parameters of the output beam at various positions relative to the principle optical axis.

Variable Position, 1.25 mm \varnothing	Input $P_1 = 0.999471(5)$	Input $P_2 = -0.000546(11)$	Input $P_3 = 0.001354(9)$	Input $P_{tot} = 0.999472(5)$
	P_1 Output	P_2 Output	P_3 Output	P_{tot} Output
12 o'clock	0.039005(1597)	-0.031269(1568)	0.013392(804)	0.051755(2359)
3 o'clock	-0.030366(1450)	-0.045266(1426)	-0.014372(656)	0.056370(2093)
6 o'clock	0.013130(959)	0.025267(943)	-0.000282(482)	0.028477(1284)
9 o'clock	0.043433(1242)	0.011162(1265)	0.011340(620)	0.046256(1624)
center	0.030657(1014)	-0.029741(1029)	0.006465(518)	0.043200(1505)

state of the output light of this diffusion-based depolarizer is isotropic across the beam cross section.

C. Intensity attenuation

The depolarizer described here is capable of producing light that is well less than 1% polarized when integrating across the full 15-mm diameter of the output beam. However, because the primary depolarizing elements are diffusers, the loss of intensity of the transmitted beam needs to be considered. Comparing the throughput intensity recorded by the photodiode without the depolarizer in the optical train (i.e., when measuring the input polarization state) to the throughput intensity when the depolarizer was present provides a measure of the transmission efficiency of the depolarizer. This attenuation is quantified as the ratio of the signal that

reaches the photodiode when the depolarizer is present to that which reaches the photodiode when it is not. This ratio is shown for select configurations in Table V below (“Fraction Transmitted”).

Clearly, incident light is highly diffused by the depolarizer. Even for the case corresponding to the greatest percentage of transmitted light (150-W bulb and opal diffuser), only 0.484% of the light entering the depolarizer is transmitted to the photodiode on the principle axis. Given the generally low transmission efficiency of the device, it is important to show that the final collimated beam emerging from the depolarizer is usable in an experiment, i.e., that the throughput light reaching the photodiode is sufficiently greater than the background signal. To measure this signal-to-noise ratio, we determined the photodiode signal when the depolarizer was in place both before and after a beam block was inserted immediately downstream of the depolarizer. The configuration that

TABLE V. The fraction of the light that enters the depolarizer and is detected by the photodiode as well as the signal-to-background ratio for select depolarizer configurations.

Light Source	Depolarizing Element	Cavity	Fraction Transmitted	Signal to Background
640-nm Laser (linear input)	Opal	PTFE	3.28×10^{-5}	28.0
	Ground	PTFE	1.79×10^{-3}	1540
	Broadband	PTFE	1.16×10^{-5}	9.73
	Opal	PTFE w/ Kimwipe®	2.30×10^{-7}	0.124
	Opal	Stained PTFE	2.18×10^{-5}	13.9
	Sandblasted Opal	Stained PTFE	1.80×10^{-5}	11.5
405-nm Laser (linear input)	Opal	PTFE	3.44×10^{-5}	0.749
	Opal	Stained PTFE	1.82×10^{-5}	0.368
	Sandblasted Opal	Stained PTFE	1.65×10^{-5}	0.350
150-W bulb with 640-nm Filter	Opal	PTFE	4.84×10^{-3}	118
	Sandblasted Opal	PTFE	4.67×10^{-3}	53.8
	Opal	Stained PTFE	1.77×10^{-3}	20.3
	Sandblasted Opal	Stained PTFE	2.07×10^{-3}	21.3

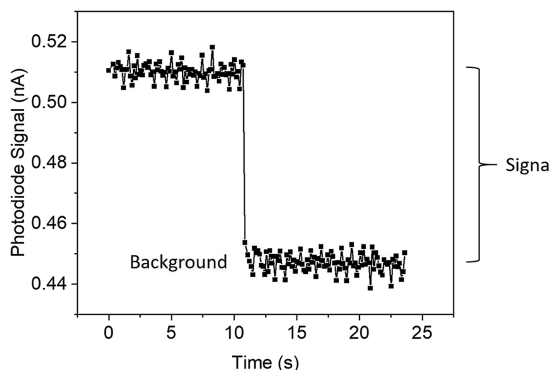


FIG. 4. Signal (no beam block) and background (beam blocked immediately downstream from the depolarizer) when the depolarizer, using opal disks and Kimwip®-filled cavities, is in the optical train shown in Fig. 2.

attenuated the intensity the most, the Kimwip®-filled depolarizer, only allowed 2.30×10^{-5} percent of the input light through. Figure 4 shows the signal and background measured for this configuration. Even in this case, the signal is still clearly identifiable above the background.

The signal-to-background measurements such as those shown in Fig. 4 and reported in Table V show that even in its most opaque configuration, the depolarizer transmits light that is sufficiently intense to be used in an experiment.

IV. CONCLUSION

In this work, we have reported on the performance of a simple, compact, low-cost light depolarizer. The design allows for some customization by the user. The depolarizer is capable of reducing the total polarization of the input light from more than 99% to less than 1% when integrating across a diameter of 15-mm. Commercially available depolarizers produce beams of locally varying high polarization across their widths. The polarization must thus be spatially averaged over the beam cross section to be considered unpolarized. The depolarizer presented here is based on the diffuse scattering of light, and thus, all local points in the transmitted beam's cross section have relatively low polarization—less than 6%. Having said this, spatial averaging, as is the case with commercial devices, is needed to reach the lowest polarizations that the device is capable of achieving—in our case, $\sim 0.6\%$ with an input $P_{tot} \approx 1$. However, because the depolarizing elements are diffusers, the intensity of the light transmitted through the depolarizer is greatly attenuated along the optical axis. Despite this loss of intensity, we have shown that even in the most extreme case, the amount of light passing through the depolarizer along the optical axis is detectable above the background.

SUPPLEMENTARY MATERIAL

The supplementary material accompanying this work contains the complete normalized Stokes vectors and the total polarization measurements discussed throughout the manuscript.

ACKNOWLEDGMENTS

The financial support for this work was provided by the National Science Foundation (NSF) under Grant No. PHYS-2110358.

AUTHOR DECLARATIONS

Conflict of Interest

The authors have no conflicts to disclose.

Author Contributions

K. D. Foreman: Conceptualization (equal); Data curation (lead); Formal analysis (lead); Investigation (equal); Methodology (lead); Validation (equal); Writing – original draft (lead); Writing – review & editing (equal). **T. J. Gay:** Conceptualization (equal); Data curation (supporting); Formal analysis (supporting); Funding acquisition (lead); Investigation (equal); Methodology (supporting); Project administration (lead); Resources (lead); Supervision (lead); Writing – original draft (supporting); Writing – review & editing (equal).

DATA AVAILABILITY

The data that support the findings of this study are available from the corresponding author upon reasonable request.

REFERENCES

1. S. Trillo and S. Wabnitz, "Parametric and Raman amplification in birefringent fibers," *J. Opt. Soc. Am. B* **9**(7), 1061–1082 (1992).
2. K.-X. Sun, P. Lu, R. L. Byer, J. A. Britten, H. T. Nguyen, J. D. Nissen, C. C. Larson, M. D. Aasen, T. C. Carlson, and C. R. Hoaglan, "Characterization of polarization sensitive, high efficiency dielectric gratings for formation flight interferometry," *J. Phys.: Conf. Ser.* **154**, 012031 (2009).
3. T. J. Gay, J. E. Furst, K. W. Trantham, and W. M. K. P. Wijayaratna, "Optical electron polarimetry with heavy noble gases," *Phys. Rev. A* **53**(3), 1623–1629 (1996).
4. T. J. Gay, "Physics and technology of polarized electron scattering from atoms and molecules," *Adv. At. Mol. Opt. Phys.* **57**, 157–247 (2009).
5. T. J. Gay, "Accurate electron spin optical polarimetry (AESOP)," *J. Phys.: Conf. Ser.* **875**, 052043 (2017).
6. K. W. Trantham, K. D. Foreman, and T. J. Gay, "Demonstration of vacuum strain effects on a light-collection lens used in optical polarimetry," *Appl. Opt.* **59**(9), 2715–2724 (2020).
7. K. D. Foreman and T. J. Gay, "Collection of dim light for accurate optical polarimetry by a plano-convex spherical lens," *Meas. Sci. Technol.* **33**(1), 015201 (2022).
8. See <https://www.meadowlark.com/precision-achromatic-retarder/> for "Precision achromatic retarder" from Meadowlark Optics.
9. J. C. Kemp, G. D. Henson, C. T. Steiner, E. R. Powell, and E. R. Powell, "The optical polarization of the Sun measured at a sensitivity of parts in ten million," *Nature* **326**, 270–273 (1987).
10. D. J. Gambling and B. Billard, "A study of the polarization of skylight," *Aust. J. Phys.* **20**, 675–681 (1967).
11. See https://www.thorlabs.com/newgroupage9.cfm?objectgroup_id=8043 for example "Liquid crystal polymer depolarizers" from Thorlabs, Inc.
12. See <https://www.edmundoptics.com/f/lyot-depolarizers/14010/> for example, "Lyot depolarizers" from Edmund Optics®.
13. H. G. Berry, G. Gabrielse, and A. E. Livingston, "Measurement of the Stokes parameters of light," *Appl. Opt.* **16**(12), 3200–3205 (1977).
14. S. R. Scholes and C. H. Greene, *Modern Glass Practice*, 7th ed. (Cahners Books, Boston, 1975).